

Block copolymer knots

Franco Ferrari^{1*}

¹*CASA* and Institute of Physics, University of Szczecin, Szczecin, Poland*

(Dated: November 10, 2021)

An extensive study of single block copolymer knots containing two kinds of monomers A and B is presented. The knots are in a solution and their monomers are subjected to short-range interactions that can be attractive or repulsive. In view of possible applications in medicine and the construction of intelligent materials, it is shown that several features of copolymer knots can be tuned by changing the monomer configuration. A very fast and abrupt swelling with increasing temperature is obtained in certain multiblock copolymers, while the size and the swelling behavior at high temperatures may be controlled in diblock copolymers. Interesting new effects appear in the thermal diagrams of copolymer knots when their length is increased.

PACS numbers:

Polymer knots are abundant in nature and in artificial polymer materials [1–5]. They can be created in the laboratory [4, 5] and have attracted a considerable attention both from experimentalists and theoreticians of several different disciplines. When direct measurements are too difficult to be performed, numerical simulations are used to provide reliable predictions on the properties of these knots. So far, an important aspect of polymer knots has not been studied or studied marginally [10], namely that of block copolymer knots. This is the goal of the present work. The copolymer knots are defined here on a simple cubic lattice and contain only two kind of monomers, A and B . Monomers of the same kind repel themselves, while the interactions between A and B are attractive. Two classes of copolymer knots will be studied, namely the AB –diblock copolymers and the multiblock copolymers. These classes will be called $D(N_A, N_B)$ and $M(s_A, s_B)$ respectively. Here N_A and N_B denote the number of A and B monomers forming the two blocks of a AB –diblock copolymer. Of course $N_A + N_B = N$, N being the total monomer number. In $M(s_A, s_B)$ copolymers, a block consisting of s_A monomers of type A followed by s_B monomers of type B , is repeated n –times. For example, $M(2, 2)$ corresponds to $(A_2B_2)_n$ multiblock copolymers. Furthermore, homopolymer knots with N monomers subjected to short attractive and repulsive interactions will be denoted with the symbols $H(N, -)$ and $H(N, +)$ respectively.

The rationale for investigating such kind of copolymers is to obtain polymer knots with different behaviors by changing the monomer distribution. Particularly suitable to this purpose is the class of $D(N_A, N_B)$ copolymers. In this class the conformations in which the monomers A and B are close to each others are energetically favored because they have a lower energy due to the attractive interactions between the two different types of monomers. On the other side, the A and B monomers are concentrated in two distinct parts of the knot. As a consequence, for entropic reasons these low energy conformations are far less probable than those in which the A

and B monomers are mostly in contact only with themselves, especially when one kind of monomers is much more abundant than the other. The upshot is that it is possible to change the properties of $D(N_A, N_B)$ copolymer knots by varying the A/B monomer ratio $\eta = \frac{N_A}{N_B}$. In particular, in view of possible medical applications or of intelligent polymer materials containing knots, we show that the size of the knot can be tuned to a high extent. More precisely, it is possible to create polymers whose size is approximately stable over a given interval of temperatures, but changes after some threshold is reached. While homopolymer knots subjected to short-range interactions are essentially two-regime polymers, undergoing a slow transition from the compact to the swollen phase, at high values of η the $D(N_A, N_B)$ copolymer knots admit three regimes. The compact regime appears at low temperatures and is characterized by compact conformations. The attractive interactions are dominant. At intermediate temperatures, the repulsive interactions prevail and the copolymer is reaching its maximal extension, so that this regime can be called ultra swollen. At very high temperatures the interactions cease to be relevant and an entropy dominated regime begins, in which the knot is swollen. Multiblock copolymers in the class $M(s_A, s_B)$ have remarkable properties too. For example, they exhibit a transition from the compact to the swollen phase which is abrupt in comparison to that of homopolymers and diblock copolymers. Finally, the phase diagram of copolymer knots of type $D(N_A, N_B)$ becomes more complex with increasing values of N as new peaks appear in the heat capacity.

The used methodology will be now briefly explained. The monomers are located on the lattice sites in such a way that two consecutive monomers are linked together by one lattice bond. The bond length is one, so that the length of the knot is equal to N . The energy of a given knot conformation X is expressed by the Hamiltonian $H(X) = \varepsilon(m_{AA} + m_{BB} - m_{AB})$. The quantities $m_{MM'}$'s count the numbers of contacts between monomers of the kind M and M' , where $M, M' = A, B$. Let $\mathbf{R}_1, \dots, \mathbf{R}_N$

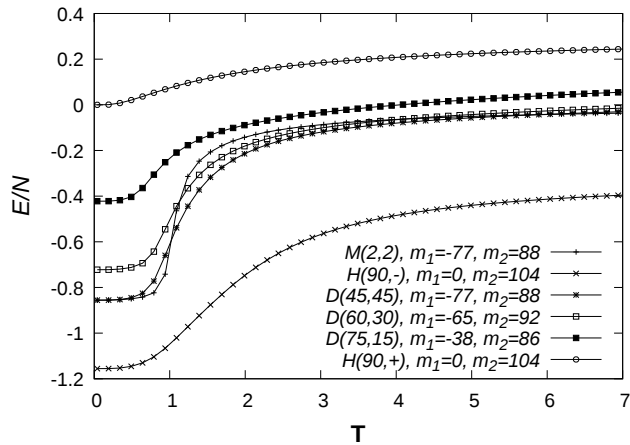


FIG. 1: The specific energy of a knot 3_1 with $N = 90$ in various monomer configurations is plotted as a function of T .

be the position of the monomers. Two monomers i and j are said to be in contact if $i \neq j \pm 1$ and $|\mathbf{R}_i - \mathbf{R}_j| = 1$. ε is the energy cost of one contact, which is positive when the A and B monomers are in contact with themselves and negative if a monomer of type A is in contact with a monomer of type B . Thermodynamic units will be assumed in which the Boltzmann constant is equal to one. For convenience, the rescaled Boltzmann factor $\mathbf{T} = \frac{T}{\varepsilon}$ and rescaled Hamiltonian $\mathbf{H}(X) = \frac{H(X)}{\varepsilon}$ are introduced. The new Hamiltonian $\mathbf{H}(X)$ takes only integer values. The simulations are performed using the Wang-Landau Monte Carlo algorithm [7]. The details on the sampling and the treatment of the topological constraints can be found in Refs. [8] and [9].

The partition function of the polymer knot is given by: $Z(\mathbf{T}) = \sum_{\mathcal{E}=m_1}^{m_2} e^{-\mathcal{E}/\mathbf{T}} \phi_{\mathcal{E}}$, where $\phi_{\mathcal{E}}$ denotes the density of states: $\phi_{\mathcal{E}} = \sum_X \delta(\mathbf{H}(X) - \mathcal{E})$. $\phi_{\mathcal{E}}$ is the quantity to be evaluated via Monte Carlo methods. The integers m_1 and m_2 define the energy interval $\mathcal{I} = [m_1, m_2]$ over which the sampling is performed. The expectation values of any observable \mathcal{O} may be computed using the formula: $\langle \mathcal{O} \rangle(\mathbf{T}) = \frac{1}{Z(\mathbf{T})} \sum_{\mathcal{E}=m_1}^{m_2} e^{-\mathcal{E}/\mathbf{T}} \phi_{\mathcal{E}} \mathcal{O}_{\mathcal{E}}$. Here $\mathcal{O}_{\mathcal{E}}$ denotes the average of \mathcal{O} over all sampled states with rescaled energy \mathcal{E} . The observables that will be considered in this work are the specific energy $\frac{E(\mathbf{T})}{N} = \sum_{\mathcal{E}=m_1}^{m_2} \mathcal{E} e^{-\mathcal{E}/\mathbf{T}} \phi_{\mathcal{E}}$, the specific heat capacity $C/N = \frac{1}{N} \frac{\partial E(\mathbf{T})}{\partial \mathbf{T}}$ and the mean square average of the gyration radius R_G^2 .

The variety of behaviors that it is possible to obtain in copolymer knots is shown in Figs. 1–3. The same trefoil knot 3_1 of length $N = 90$ is considered and only the distribution of the A and B monomers is different. From the plots of the specific energy and of the gyration radius in Figs. 1 and 3 it turns out that the homopolymer trefoil knot 3_1 has the slowest swelling rate when the temperature is increasing, independently if the interactions

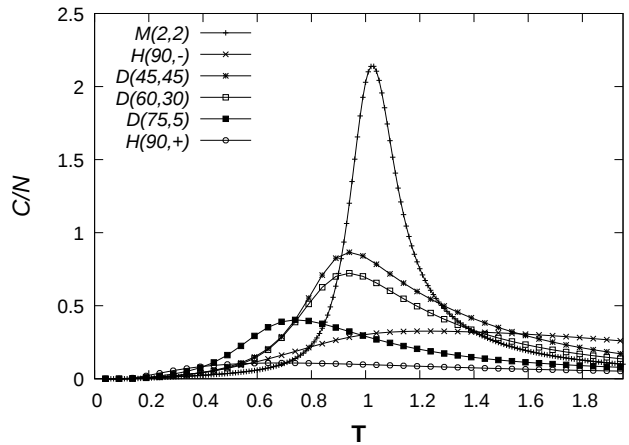


FIG. 2: The specific heat capacity of a knot 3_1 with $N = 90$ in various monomer configurations is plotted as a function of T .

are repulsive as in the variant $H(90, +)$ or attractive as in $H(90, -)$. On the contrary, the swelling process becomes abrupt in the multiblock 3_1 copolymer $M(2, 2)$. This knot undergoes a fast transition from the compact to swollen phase at $T \sim 1.2$, which causes the marked peak in the specific heat capacity in Fig. 2. This feature is present also in longer knots and persists even if the size of the blocks is increased, for instance in the case of $M(8, 8)$ copolymers. Another remarkable phenomenon appears in the plot of R_G^2 of Fig. 3. While homopolymers are simple systems whose size steadily increases with growing temperatures, the 3_1 copolymer $D(75, 15)$ exhibits a more complicated behavior. Its R_G^2 is smallest at low temperatures and increases up to its maximum value at intermediate temperatures. After that, it starts to decrease and finally stabilizes to some value between the maximum and the minimum at high temperatures. These three different regimes, compact, ultra swollen and swollen are not present in the 3_1 knot with monomer distribution $D(45, 45)$. The distribution of the A and B monomers selects also the allowed energetic states and the range of possible sizes. For example, in Figs. 1–3 the 3_1 copolymer knot $D(75, 15)$ has a lower energy limit that is bigger than that of its counterpart of type $D(45, 45)$.

One goal of this work is to investigate how the topology of a knot influences its thermal and mechanical behaviors. In the case of homopolymers it is known that topological effects are relevant especially when the knot is short and fade out with increasing length, see e. g. [9]. In $D(N_A, N_B)$ copolymers these effects are further enhanced. The reason is that cyclic AB -diblock copolymers consist of two homopolymers joined together at both ends. They look locally as homopolymers, but their global structure emerges whenever there are conformations in which a relevant number of A and B monomers

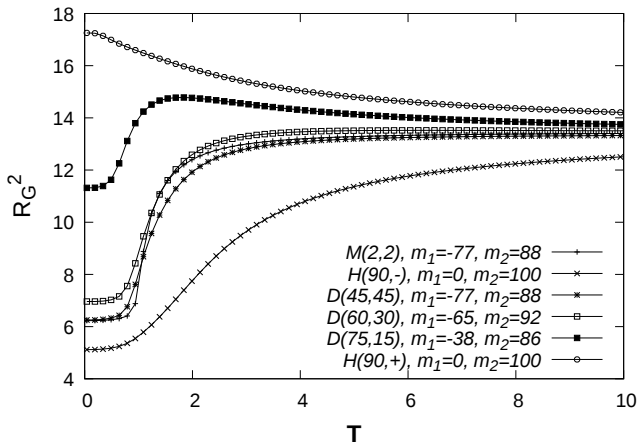


FIG. 3: The gyration radii of a knot 3_1 with $N = 90$ in various monomer configurations is plotted as a function of T .

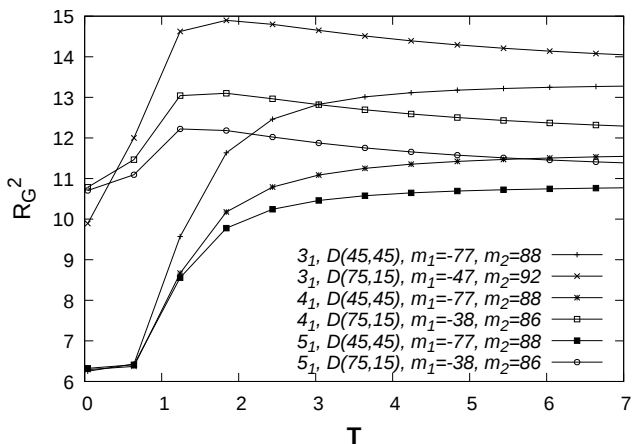


FIG. 4: Dependence of the mean square gyration radius of the knots $3_1, 4_1$ and 5_1 with $N = 90$ on the A/B monomer ratio η . Two values of η are considered: $\eta = 1$ and $\eta = 5$.

is close to each other. Since conformations of this kind are characterized by low energy values, a connection is established between the global structure of the knot, which is in turn depending on its topological properties, and conformations that are energetically favored. The plots in Fig. 4 concerning the gyration radius of a few knots of copolymer type $D(N_A, N_B)$ show that strong topological effects are at work. For example, the size of the knot 3_1 changes substantially with rising temperature in both cases $\eta = 1$ or $\eta = 5$. On the contrary, the size of the knots 4_1 and 5_1 is bound to vary within a much narrower interval when $\eta = 5$. The compact, ultra swollen and swollen regimes are observed only in the knots with $\eta = 5$. We remark that in Fig. 4 the gyration radii of knots differing only by the value of η converge to the same limit at high temperatures. The same convergence

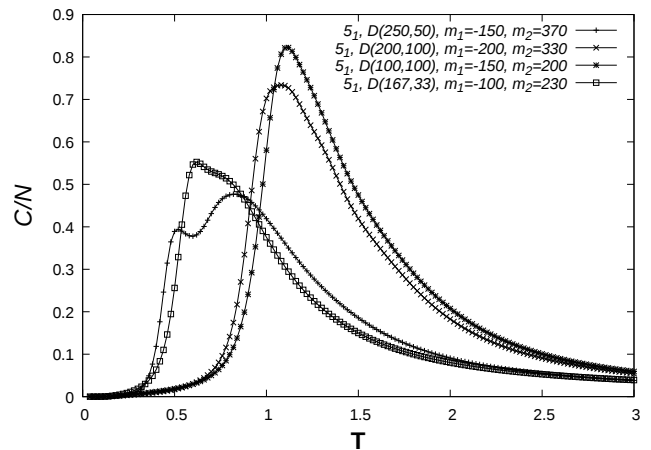


FIG. 5: Plots of the specific heat capacity of a diblock copolymer knot 5_1 with length $N = 300$ in three different monomer configurations corresponding to $\eta = 1, 2, 5$. The fourth plot displays the heat capacity of a knot 5_1 with $N = 200$ and $\eta = 5$.

is present also in Fig. 3. This is expected from the fact that, at high temperatures, the short-range interactions become irrelevant due to strong thermal fluctuations.

As already discussed, energetically favorable conformations in which the A and B monomers are close to each other are sensitive to the global properties of the knot and thus to its topology. It is therefore licit to expect the existence of an interplay between monomer distributions and topology. To show that, diblock copolymers in the knot configurations $3_1, 4_1, 5_1$ and 9_1 have been studied varying their lengths and A/B monomer ratios. The performed analysis points out that by increasing the knot topology or the A/B monomer ratio η , similar results are produced. For instance, relevant changes in size comparable to those found in the knot 5_1 with $N = 90$ when passing from $\eta = 1$ to $\eta = 5$, see Fig. 4, can be obtained also when the length is increased to $N = 216$, but only after switching to more complex knots, such as the knot 9_1 . In the topologically simpler knot 3_1 with $N = 200$, the size differences at any given temperature are not so relevant. The situation changes if in the knot 3_1 with $N = 200$ the parameter η is further increased. In order to give a rough estimation of the scale of the change, we take into account the maximum value of the mean square average of the gyration radius $R_{G,max}^2$. When $\eta \sim 7.7$ we find that $R_{G,max}^2 \sim 42.63$. This point of maximum is observed at a temperature corresponding to $T \sim 2.64$. When $\eta = 1$, instead, the quantity R_G^2 steadily increases with rising temperatures and attains its maximum value of $R_{G,max}^2 \sim 37.32$ in the upper limit $T = 20.00$ of the studied interval of temperatures. The data also indicate that the fading out of the influence of topology on the knot behavior is not so fast as in homopolymers. The

details of these calculations will be reported elsewhere.

Another interesting aspect of copolymer knots is related to the effects occurring when the length N is increased. When $N = 90$, we have seen in Figs. 1–4 that there is a swelling phase, followed by a relevant decrease of the knot size provided the topological complexity or the A/B monomer ratio are big enough. Even if the values of m_1 and m_2 are pushed almost at the limits of the range of allowed energies, the specific energy of copolymer knots with length $N < 200$ and homopolymer knots up to $N = 2100$ is always characterized by a single peak. The situation is different when longer copolymers are considered at high values of η . For example, the knot 5_1 with $N = 300$ and $\eta = 5$ exhibits in Fig. 5 a smaller peak besides the main one, which corresponds to the swelling process. This secondary peak appears at very low temperatures and is quite narrow. It is probably related to the transition from rare, very compact states. In the remaining plots shown in Fig. 5 the specific heat capacities of a 5_1 knot with $N = 300$ and $\eta = 1, 2$ and of a 5_1 knot with $N = 200$ at $\eta = 5$ are shown. No second peak has been observed in these two cases.

The simulations presented in this paper have required the sampling of an extensive amount of knot conformations. This has been possible thanks to the introduction of some improvements that have sped up considerably the original Wang-Landau algorithm. The major problem to be solved is that of rare events, see [9] and references therein. Some of the conformations appear after several hundreds of billions of trials and their inclusion would extend enormously the time of the calculations. The basic idea is to leave open the energy range while requiring the flatness condition of the energy histogram, which is crucial in the Wang-Landau algorithm, inside some definite energy interval $\mathcal{I} = [m_1, m_2]$. If the sampling process is trapped in some rare conformation outside \mathcal{I} , where a precise account of the statistics of the events is not relevant, it is easy to get rid of this difficulty. Inside \mathcal{I} , instead, the sampling of the conformations, including rare states, is made faster by introducing a two-step sampling procedure, in which during the first step the so-called modification factor becomes a function of the energy.

It should be noted that the expectation values of the observables are sensitive on the choices of m_1 and m_2 . The energy cut-off m_1 plays a key role in the study of low temperatures, where low energy conformations are preferred. At very high temperatures, instead, the results are quite independent of the values of m_1 and m_2 . The reason is that at very high temperatures the knot conformations are swollen and their number of contacts is much higher than m_1 and much lower than m_2 . To avoid biases due to a poor choice of the cut-offs m_1 and m_2 which eliminates statistically relevant conformations, the energy interval $\mathcal{I} = [m_1, m_2]$ is extended gradually, until the measured values start to converge to some limit and do not change substantially after a further extension

of \mathcal{I} . In Fig. 6 the plots of the mean square gyration radius of a knot 7_1 for increasing energy intervals \mathcal{I} are reported. These plots provide just an example of a trend which is general. First of all, as previously explained, the results at low temperatures are mostly affected by the choice of m_1 . Secondly, even if the relatively relevant part of the lower energy spectrum is neglected, see the plot in the worst case $m_1 = -60, m_2 = 60$, the data at very high temperatures are reproduced with great precision. Let us note that the measurement of the gyration radius is particularly difficult, because it is necessary to have a good statistics for each allowed value of the energy. The agreement of the plots analogous to those of Fig. 6, but drawn in the case of the specific energy, is nearly perfect. It turns out the most important features of the behavior of a polymer knot are largely independent of the values of m_1 and m_2 . For instance, from all diagrams of Fig. 6 it is possible to obtain a good estimation of the swelling rate of the knot with increasing temperatures. This allows to predict if the transition from the compact phase to the swollen phase occurs abruptly in a small interval of temperatures or slowly over a wider range of temperatures. Even the lowest resolution plot of the gyration radius in Fig. 6 allows to conclude that in a copolymer knot 7_1 of monomer configuration $D(45, 45)$ and length $N = 90$ the ultra swollen regime is not present.

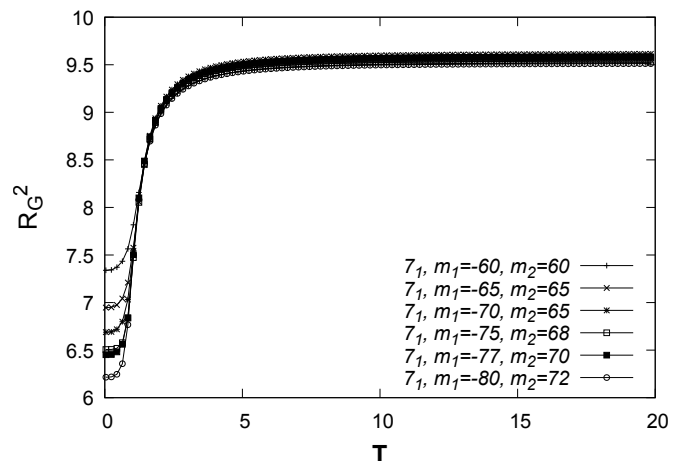


FIG. 6: The gyration radius R_G^2 of the knot 7_1 with $N = 90$ and copolymer type $T_1(45, 45)$ is plotted for increasing widths of the considered energy interval \mathcal{I} .

The simulations reported in this work were performed in part using the HPC cluster HAL9000 of the Computing Centre of the Faculty of Mathematics and Physics at the University of Szczecin. The work of F. Ferrari results within the collaboration of the COST Action TD 1308. The use of some of the facilities of the Laboratory of Polymer Physics of the University of Szczecin, financed by a grant of the European Regional Development Fund

in the frame of the project eLBRUS (contract no. WND-RPZP.01.02.02-32-002/10), is gratefully acknowledged.

* Electronic address: franco@feynman.fiz.univ.szczecin.pl

- [1] *Molecular Catenanes, Rotaxanes and Knots, A Journey Through the World of Molecular Topology*, J. P. Sauvage, C. Dietrich-Buchecker (Eds.), (Wiley-VCH Verlag, Weinheim, 1999).
- [2] J. Arsuaga, J. Roca and D. W. Sumners, *Topology of viral DNA*, in *Emerging Topics in Physical Virology*, P. G Stockley and R. Twarock (Eds.), (Imperial College Press, London, 2010).
- [3] G. Gil-Ramirez, D. A. Leigh and A. J. Stephens, *Catenanes: Fifty Years of Molecular Links*, *Angewandte Chemie International Edition* **54** (21) (2015), 6110.
- [4] J.-P. Sauvage and D. B. Amabilino. *Templated synthesis of knots and ravel*s, in *Supramolecular Chemistry: From Molecules to Nanomaterials*, P. A. Gale and J. W. Steed (Eds.), (Wiley Online Library, 2012).
- [5] *Topological Polymer Chemistry*, Y. Tezuka (Ed.), (World Scientific, Singapore, 2013).
- [6] W. Wang, Y. Li and Z. Lu, *Science China Chem.* **58** (9) (2015), 1471.
- [7] F. Wang and D. P. Landau, *Phys. Rev. Lett.* **86** (2001), 2050.
- [8] Y. Zhao and F. Ferrari, *JSTAT J. Stat. Mech.* (2012), P11022.
- [9] Y. Zhao and F. ferrari, *J. Stat. Mech.* (2013), P10010.
- [10] In Ref. [6] a particular kind of multiblock copolymers with a fixed length of forty segments has been investigated, which does not sustain the remarkable properties found in the longer copolymers studied here.